ISSN 0915-633X

NATIONAL INSTITUTE FOR FUSION SCIENCE

Mesh Effect in a Parallel Plate Analyzer

Y. Hamada, Y. Kawasumi, H. Iguchi, A. Fujisawa, Y. Abe
and M. Takahashi

(Received – Oct. 26, 1992)

NIFS-203 Dec. 1992

RESEARCH REPORT
NIFS Series

NAGOYA, JAPAN

Mesh effect in a parallel plate analyzer

Y. Hamada, Y. Kawasumi, H. Iguchi, A. Fujisawa,
National Institute for Fusion Science, Nagoya,
464-01,Japan

Y.Abe and M.Takahashi
Faculty of Engineering, Iwate University, Morioka,
020, Japan

Abstract. The effect of field irregularity due to meshes on the holes of a lower electrode in a parallel-plate electrostatic analyzer for beam penetration, is experimentally and numerically investigated. Displacement of a focal point and degradation of analyzer characteristics are found in the experiment. They are also confirmed by numerical analysis. Criteria for the error estimation are theoretically derived and found to be consistent with the experiment.

Keywords, analyzer, mesh, deflection, HIBP, focus,

§1 Introduction

Since a parallel-plate electrostatic analyzer[1] and a cylindrical mirror analyzer[2] have the focus of the second order, their resolution can be intrinsically very high. The effect of beam deflection by the field irregularity due to holes in a base electrode for beam penetration, must be, therefore treated carefully in order to get high resolution in an energy analyzer. In order to reduce the effect of holes, the diameter of the holes must be small or fine meshes are usually placed on the holes. In the following cases, where a large entrance angle of the beam or a wide input-slit is required, which means larger holes are required, the effect of meshes is essential for a measurement of particle energy with high resolution.

In order to detect a fine change of beam energy, the effect of collisions of particles with a mesh on holes, that is a shadow effect of the mesh, and the deflection of a beam due to field irregularity at a mesh, must be minimized. In a case of a fine mesh(20 wires/1mm for example), it must be matrix-typed because of the mechanical stability and rigidity. It has therefore, very low transparency at an entrance angle of 30 degrees due to the finite thickness of the mesh. In addition, local fields near wires perpendicular to the axis of the detector cause small deflection in beam trajectories and induce errors in the measurement of small changes of the energy. Accordingly, a fine mesh may not be appropriate for a measurement with very high resolution.

A rather rough mesh with wires parallel to the axis of an analyzer does not suffer so much from the error due to the deflection of a beam in the analyzer plane in a measurement of the energy of particles and has very high transparency. It is appropriate for the measurement of fine change of the energy, but it has also a shadow effect if wires are placed densely and the error due the deflection of a beam into the direction perpendicular to the analyzer plane. Accordingly, we have to make an appropriate choice of a mesh. Data of analyzer characteristics of various meshes are, therefore, very valuable.

Most of the previous discussions on the effect of holes at the electrodes are limited to the effect of two-dimensional slits, because the electric field in this case can be rigorously solved by the confocal mapping[3] or expressed in the recursion formulas[4]. In case wide in-plane and out-of-plane injection angles are needed, we have to use a number of fine wires as meshes on large holes instead of simple rectangular holes for the entrance and exit of the particles. In this case exact mathematical formulas are difficult to obtain as a two-dimensional problem.

The effect of circular holes in a cylindrical mirror analyzer is theoretically discussed by L.Frank[5]. He found

that a focal point shifts due to the deflection of field irregularities near the holes. In this experiment, a large displacement of a focal point in a parallel-plate analyzer and the disappearance of the second-order focus properties, are observed even in the case of long wires on large holes. These effects can not be explained in the 2-dimensional analysis. In addition, three dimensional numerical analysis is performed and qualitative agreement between the numerical computation and the experiment is observed for these effects. These results are very useful in the design of meshes of a parallel plate analyzer for a precise measurement of the energy of particles emitted from extended source.

$ 2 Experimental setup

The analyzer used in this experiment is a parallel plate analyzer with 30 degrees entrance angle[1]. Its schematics and its physical size are shown in Fig. 1[6]. It is designed to analyze a change of the energy of doubly ionized thallium beam from the original energy of a singly ionized beam injected into JIPP T-11U tokamak[7] as a part of the heavy ion beam probe(HIBP). The injected thallium beam has the energy up to about 0.5 MeV. The amount of the change of the energy corresponds to a local electric potential in a plasma where ionization takes place[8]. The doubly ionized thallium hits an entrance slit of the analyzer at different positions and different entrance in-plane and out-of-plane angles as the place of the ionization is swept across the plasma to get a potential profile of the plasma.

It has a shaped upper electrode instead of guard rings with a resistor chain in order to get very uniform electric field[6,9,10]. Due to the photo-electron flow into the guard rings under the intense irradiation of UV, VUV and soft x-ray from hot plasmas, potentials of the guard rings with a resistor chain changed considerably and a large deformation of the electric field was observed in an

analyzer of HIBP at TEXT tokamak[10]. Reduction of the resistance for reducing this effect causes, however, a serious problem of large heat generation in the resistors which are placed at a very high potential in the vacuum. A shaped electrode system is one of the solutions to avoid these problems. The vacuum vessel serves as a boundary of the electrostatic potential. The diameter of a coronal ring is numerically optimized for the maximum uniformity of the field.

The detector is composed of two plates parallel to a input slit. From a ratio of ion currents on the plates, beam position and a small change of the energy is deduced. In order to tune the detector to a focal point, it is mounted on a precision slide-mount which slides in a plane inclined by 30 degrees to the parallel plate. In addition, the whole analyzer can be tilted in two directions in order to scan in-plane and out-of-plane entrance angles of the beam to the analyzer while the center of the input slit is kept as a fixed point.

One of main characteristics of an analyzer is how a beam position on the detector plates changes as a function of an in-plane and an out-of-plane entrance angles of a beam. It is conveniently described by a gain function of an analyzer[11]. The gain is a ratio of the beam energy in the unit of electron volt to the analyzer voltage when a beam hits just the middle between an upper and a lower detector plates. The designed value of the gain of our analyzer for doubly ionized particles is 5 at the injection angle of 30 degrees. Theoretical gain curves with various distances(d) of the detector plates from the center of the exit hole, are simply described by a equation,

$$G(\theta,\varphi)=\frac{Q_b}{2H_1}\ \frac{L_t+(d-h_f/\sin\theta_o)\cos\theta_o-(h_i+d\cos\theta_o)\cot\theta}{\sin 2\theta\cos^2\varphi}\ , \qquad (1)$$

where θ is an in-plane entrance angle and θ_0 is the entrance angle of 30 degrees, which is the angle of the

2nd-order focussing. Q_b is the charge number. φ is an entrance angle perpendicular to the plane of analyzer. Other quantities are shown in Fig. 1 and 2. The dependence of gains on an in-plane entrance angle are shown in Fig. 3. Since a focal point is the point where the derivative of gain with an entrance angle is zero, we can see in Fig. 3 that at a little smaller d(distance of detector), the analyzer has two focal points of the first order. As d becomes larger two focal points merge and become the second-order focal point.

In this experiment, a 7 keV rubidium beam is injected into the energy analyzer for the check of the performance of the analyzer. Its trajectory lies almost on the symmetry plane of the analyzer in order to check solely the effect of the mesh. The size of the rectangular holes on the lower plate is 4 cm wide and 8 cm long along the trajectory of the beam for the entrance of the beam, and 10 cm wide and 8 cm long for the exit of the beam. In order to reduce the irregularity of the field due to those holes and to avoid a shadow effect of meshes, wires with diameter of 0.1 mm are welded in the z direction(along the analyzer axis) every 2 cm apart (case 1), every 5 mm apart(case 2) and wires along the x direction(perpendicular to the analyzer axis) with every 3 mm distance(case 3).

§3 Experimental results.

In the experiment, a injected beam is fixed and the analyzer is rotated in order to scan an entrance angle of the beam. During this scan the beam energy and the analyzer voltage are fixed. The shift of a beam on the detector plates is estimated by a ratio of currents on the upper and lower plates by the method discussed by Solensten and Connor[11]. The shift of the beam on the detector plates agrees well with a simple theoretical estimate when an analyzer voltage is changed by a small amount. The gain function can be easily obtained as a function of an entrance angle of the beam.

The measured gain function in case 1(wires 20mm apart) is shown in Fig.4. The shift of a focal point is found to be as large as about 4.8 cm in this case. Figure 5 shows the gain curves in the case 2 (5mm apart). In this case the shift is about 1.9 cm. It is clearly shown that the shift of a focus point depends on the distance between the wires. When the wires are closer together, a focal point approaches to the theoretical one.

The deflection by field irregularities at the wires is clearly observed, as is expected, when the direction of wires is changed from parallel to the analyzer axis to perpendicular to the axis of analyzer. In this case the dominant deflection of a beam is in the plane of an analyzer. Figure 6 shows beam currents of upper and lower plates as functions of an in-plane entrance angle of the rubidium beam in the case where wires are 3mm apart and perpendicular to the analyzer plane(case 3). Since the height of the input slit is 2 mm, the detector system(upper and lower plates) is very sensitive to beam movement in the analyzer plane. In Fig.6 we can clearly observe large and rather regular ripples in the currents on the upper and lower plates. Those fluctuate out of phase as a function of an in-plain entrance angle, meaning that it is due to the deflection of the beam by the local field near the wires on the entrance and exit holes. If it is simply due to shadows of meshes, the ripples of the currents should be in-phase.

§4 3-dimensional numerical calculation

The 3-dimensional finite difference code with rectangular grids and various grid distances, is used in order to study the effect of field irregularity due to wires. For simplicity the model analyzer is a rectangular box with an upper high voltage plate and a middle earth plate with holes and meshes and a bottom earth plate. As a boundary condition, the electric field is perpendicular to the side plates. The error due to this simplification is considered to be negligible and the effect of the wires

will be clarified, since the beam trajectory in the experiment is confined near the symmetry plane of the analyzer and the diameters of the entrance and exit holes are much smaller than the distance between the side plates. Figure 7a, b show contours of the electric potential along the x axis, at the middle of the entrance and exit holes in case 1. Figure 7c shows the contours on the symmetry plane of the energy analyzer in case 1. The concave equipotential lines at the input and exit meshes in Fig. 7c induce a shift of a focus point, while concave lines in Fig. 7a and 7b deflect a beam into the direction perpendicular to the analyzer plane.

Trajectories of the beam is calculated by Runge-Kutta-Gill method. The expanded view of the trajectories near a focal point in case 1 is shown in Fig. 8. A very large shift of a focal point is clearly observed in the simulation, but the numerical computation gives nearly a half of the shift observed in the experiment. The difference in these shifts may be ascribed to the modelling in a finite difference code. In the code, a wire is simulated only by fixing potentials of a train of grid points on the wire at the earth potential. Although the distance between the grids around wires is reduced to as small as 1 mm, it is much larger than the diameter of the wires. The wires used in the experiment have the diameter of 0.1 mm in order to reduce shadow effect. Since a potential changes considerably near the wires, this modelling may induces errors and the difference in the shift of a focus point. These errors may be reduced if we reduce the distance of the grid points in the finite difference method to about the radius of the wires. However, because of the huge increase in the memory region of the program, we could not run the program under this condition.

The precise behaviour of the focussing properties is observed in the gain curve of the analyzer. The calculated gain curves for case 1 and 2 is shown in Fig. 9a and 9b. In fig. 9a we can also observe that the displacement of a

focal point is about 2 cm in the numerical simulation. In addition, when we compare gain curves in the ideal case(Fig 3) to those of case 1, we can observe that the second-order focus disappears . In the ideal case, this analyzer has two focal points of the first order at smaller d(distance of detector) and they merge at certain d. These trends disappear due to the effect of field irregularity at the wires as shown in Fig.9a.

When we increase the diameter of the holes along the analyzer axis on a lower electrode and increase the length of wires keeping the distance between wires constant, the amount of the shift of a focal point decreases. This means that the shift of a focal point is due to the deflection of the beam in the analyzer plane and is not due to weakening the effective field intensity due to the holes.

Another feature in Fig. 9a,b is that the gain curves merge at the same value at 30 degrees in the numerical simulation, while in the experiment, gain curves do not merge.at one entrance angle. In order to explain these differences, the simulation code with more sophisticated boundary may be required.

The dependence of the shift of a focal point on the distance of wires of meshes is shown in Fig. 10. As the distance becomes smaller, the focal point numerically obtained approaches the theoretical focal point.

§5 Discussions

As is experimentally and computationally shown, the distance between wires on the holes has a large effect on the behaviours of a parallel plate analyzer. The distance between wires parallel to the analyzer plane should be determined by the error of the energy due to the deflection of the beam by the wires into the plane perpendicular to the analyzer plane. The wires perpendicular to the analyzer plane induce large error as shown in Fig.6. Since the precise evaluation of the optics of a mesh is rather difficult, we want to derive the optics of a hole(circular

and 2-dimensional) or a slit with arbitrary injection angle in order to get a rough estimate of the deflection angle of a mesh.

The lens effect of a slit parallel to the analyzer axis in the case of perpendicular injection is a standard problem[12] and focal length can be described by

$$f=\frac{2.0V_b}{Q_bE}=H_1\frac{2.0V_b}{Q_bV_a} \qquad (2),$$

where Q_b, and V_b are the charge number and the energy of the beam in the units of electron volt. E is an electric field between parallel plates. In the case of the in-plane entrance angle θ, the focal length will be modified to

$$f=H_1\frac{2.0V_b}{Q_bV_a}\sin^2\theta \qquad (3),$$

because the beam energy in the xy plane is $V_b\sin^2(\theta)$.

In the case of the beam deflection into the out-of-plane direction by a slit parallel to the axis of the analyzer, the maximum deflection angle($\Delta\varphi$) of the beam due to the slit or a hole is given by $\Delta\varphi=a/2f$ where a is the opening of a slit or a hole. The error in a measurement of an energy, ΔV_b due to the deflection is given by

$$\Delta V_b=V_b\sin^2(\theta)(a/2f)^2, \qquad (4),$$

since the energy measured by an energy analyzer is from the velocity along the analyzer plane.

A lens effect of a slit perpendicular to the analyzer axis, is a little complex problem and may be obtained by following the method discussed by L.Frank. It is found that the focal length is the same for the case with a slit parallel to the analyzer plane.

The error in a measurement of an energy induced by this slit may be derived in the following way. The

deviation of the cross point on the detector plates at the ideal focus due to the lens effect of an exit slit, may be given by $h_f\cot(\theta)\Delta\theta$, where $\Delta\theta = \sin(\theta)a/2f$, if the intrinsic deviation is assumed to be negligible because θ is near 30 degrees and a parallel plate analyzer has good focussing properties of the 2nd-order. The deviation due to a lens effect of an input slit is $h_i\cot(\theta)\Delta\theta$ by a similar discussion. The maximum deviation may be the sum because we want to simulate the case where there are actually many small slits in exit and input holes and these effect are random in phase. The error in the energy can be determined by the total deviation on the detector plate and the energy dispersion. The error in an energy may be given by

$$\Delta V_b = V_b\left(\frac{Q_b V_a}{V_b}\right)^2 \frac{a(h_i+h_f)\cot(\theta)}{8H_1^2\sin 2\theta} \qquad (5).$$

Compared to the case with a slit parallel to the analyzer plane, the effect of a slit perpendicular to the analyzer plane is quite large as shown in Fig. 6, because ΔV_b is proportional to a/H_1 instead of $(a/H_1)^2$ in equation 4. We have to use a very fine mesh to reduce this effect in spite of the very low transparency at the entrance angle of 30 degrees, or wires parallel to the analyzer plane. The error reduced by equation 5 and the one obtained in Fig. 6 agrees within factor 2. Accordingly, these equation serves as rough criteria for estimating errors in a parallel plate analyzer with wires on the holes.

The equation of focal length of a circular hole in the parallel plate analyzer can be estimated from the discussions at cylindrical mirror analyzer[5] and can be written in the form

$$f = H_1\frac{4.0V_b}{Q_b V_a}\sin^2\theta \qquad (6).$$

The actual focal lengths derived by equation 3 and 6 are $1.25H_1$ for a slit and $2.5H_1$ for a circular hole in case of the entrance angle of 30 degrees and the analyzer gain of 5 for doubly ionized particles. Since these distances are smaller than the total length of the trajectory in the analyzer it can be easily understood that a hole or a slit has a large effect on the focussing properties of the analyzer. The main feature of these equations is that a focal length is independent of the opening distance of a slit or the diameter of a hole. Accordingly, the reduction of these effect may be obtained by the use of a very small hole or a very fine mesh on a large hole. Another solution is the use of wires parallel to the axis of the analyzer on a hole, taking into consideration the error due to deflection into out-of-plane direction and a shift of a focal point. In this experiment, a ratio of the distance of wires parallel to the axis to the distance between wires is about 4 in case 1. It still has large defocusssing properties. In case 2, the ratio is 16 and the change of analyzer characteristics is small.

§6 Summary

In order to reduce a lense effect due to holes in an electrostatic parallel plate analyzer or a cylindrical mirror analyzer, fine meshes may be commonly used for input and exit holes of a lower electrode. Fine meshes are, however, must be matrix-typed in structure and therefore have very low transparency due to finite thickness in case of an entrance angle of 30 degrees. In addition, it also induces small energy ripple due to wires perpendicular to the analyzer axis. Accordingly, a group of wires parallel to the analyzer axis on the holes may be the best choice for the extended source. In this case, the optimization between the reduction of a shadow effect of the wires, a displacement of the focal point, change of the analyzer characteristics and the error induced by the deflection of

a beam into out-of-plane direction, must be performed. In this study, some data and design criteria for the selection of distance between wires in a parallel plate analyzer, which has a wide in-plane entrance angles and a slit with large entrance width, are presented.

Acknowledgement

We express sincere gratitude to Director A.Iiyoshi and Prof. M. Fujiwara for continuous supports. This work is performed as a part of the development of 500keV heavy ion beam probe for JIPP T-IIU tokamak. Data acquisition and analysis are performed by the data acquisition system of JIPP T-IIU. We are indebted to Mr. Haba for electronics of our apparatus.

Reference

1)T.S.Green and G.A.Proca, Rev.Sci.Instrum.**41**,1409(1970).
2)V.V.Zashkvara, M.I.Korsunsii, and O.S.Kormache, Soviet Physics-Technical Physics **11**,96(1966).
3)G.A.Proca and C.Rudinger, Rev.Sci.Instrum.**44**,1381(1973)
4)G.Bosi, Rev.Sci.Instrum.**43**,475(1972).
5)L.Frank, J. Phys. E: Sci. Instrum **9**,670(1976).
6)Y.Hamada, Y.Kawasumi, M.Masai, H.Iguchi, H.Fujisawa, and JIPP T-IIU Group, Rev,Sci.Instrum. **63**, 4446(1992).
7)K.Toi, Y.Hamada, et al.,in Plasma Physics and Controlled Nuclear Fusion Research 1990,Vol. 1,,301,IAEA, Vienna (1991).
8)J.C.Jobes, and R.L.Hickok, Nuclear Fusion **10** 195(1970).
9)P.E.McLaren,K.A.Connor,J.F.Lewis, R.L.Hickok, T.P.Crowley, J.G. Schatz and G.H. Vilardi, Rev. Sci. Instrum. **61**,2955(1990).
10)P.M.Schoch,A.Camevali,K.A.Connor,T.P.Crowley, J.C.Forster, R.L.Hickok,J.F.Lewis, and J.G.Schatz,Jr, Rev,Sci.Instrum. **59**,1646(1988).
11)L.Solensten and K.A.Connor, Rev.Sci.Instrum. **58**,516

(1987).
12)J.R.Pierce, Theory and design of electron beam, D.Van Nostrand Co., Inc. New York (1954)

Figure Captions

Fig. 1. Schematics of a parallel plate analyzer used for this experiment. a) a cross-sectional view. Y axis is the axis of symmetry and lies in an analyzer plane. b) a side view of the analyzer. The detector moves along the dashed line (30 degrees from the plane of electrode) on a precision slide mount. H_1 = 10cm, H_2 = 7.5cm, A_V = 25cm, S_1 = 15cm. A_V = 1.675cm.

Figure 2.

Beam trajectory in a parallel plate energy analyzer. It also shows notations of various parameters of the analyzer. (L_t, h_f) is the ideal second-order focus point. L_t = 64.95cm, h_f = 7.5cm. h_i = 10cm. A dashed line shows the slope on which the detector slides on the precision slide mount. The position of a detector is measured by the distance(d) from the center of an exit hole on the detector slide plane.

Fig. 3. Gain functions of an ideal parallel plate analyzer at different positions of the detector plates (d). d= 10cm is a theoretical focal point of the second order. d is changed from 9.25cm to 11cm by a step of 0.25cm.

Fig.4. Experimentally obtained gain functions with different position of the detector plates. Wires are 2cm apart(case 1). The position is measured by the distance from the center of an exit hole along 30 degrees slope to the electrode.

Fig.5. gain functions with different position of detector plates. Wires are 5 mm apart(case 2).

Fig.6. Detector currents versus in-plane entrance angle in the case where wires of meshes on input and exit holes are perpendicular to the analyzer plane and 3 mm apart (case 3). a) a current on the upper plate. b) a current on the lower plate.

Fig.7. Equipotential lines calculated at various cross-sections in case of wires 20 mm apart: a) contours of potentials in the plane perpendicular to the analyzer axis at the middle of an input hole, b) contours at the middle of a output hole perpendicular to the analyzer axis, c) contours in the analyzer plane.

Fig. 8. The expanded view of beam trajectories near a focal point in case of wires 20 mm apart. The ideal 2nd-order focus focus point is (71.1, 5.0).

Fig. 9a,b. Calculated gain functions with different position of the detector plates. Wires are 20 mm apart for fig. 9a and 10 mm apart for 9b. The position is measured by the center of the exit hole along 30 degrees slope to the electrode. The distance between wires in the input and output meshes is the same.

Fig. 10. The dependence of the calculated shift of a focal point on the distance between wires.

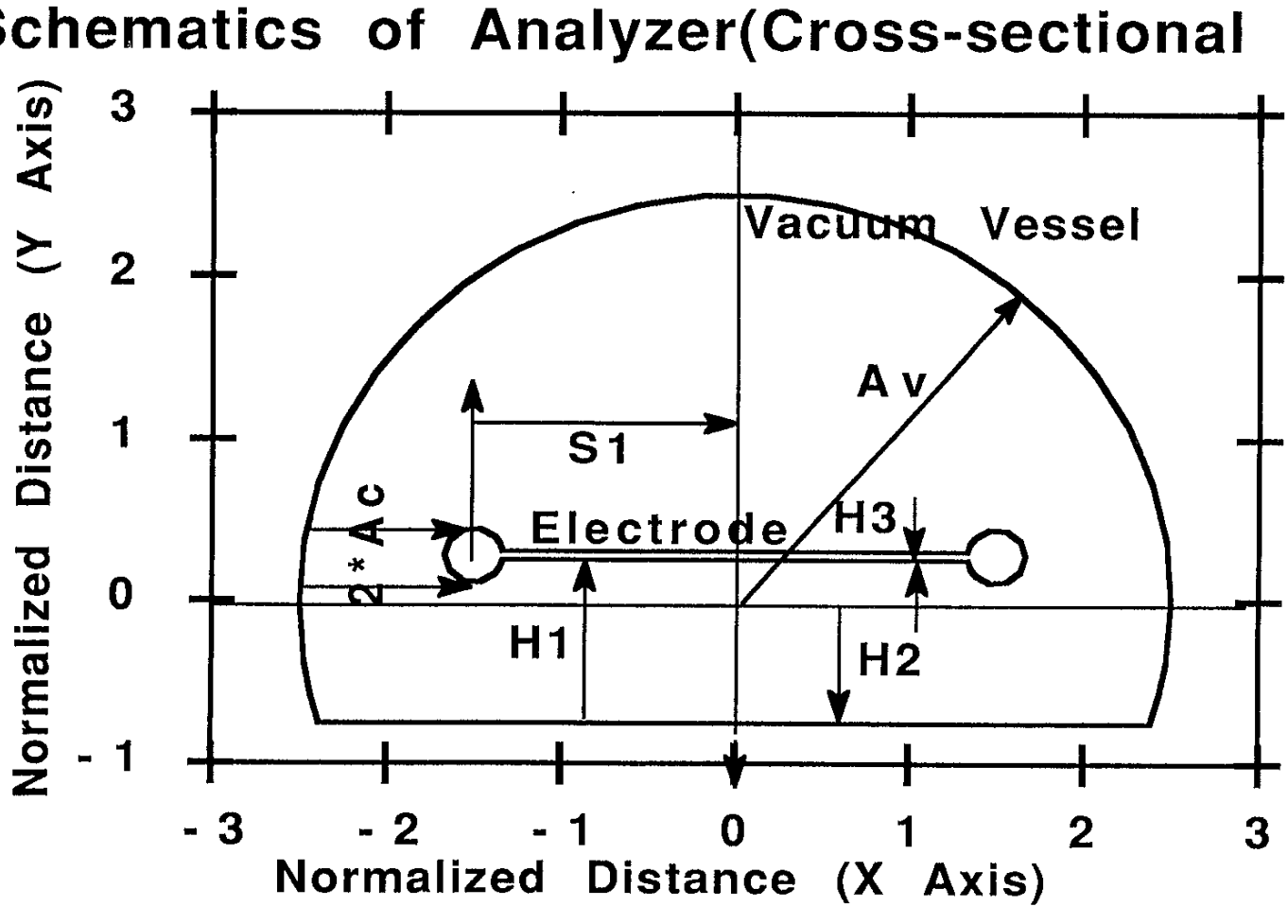
Schematics of Analyzer(Cross-sectional View)
Normalized Distance (Y Axis)
3
2
1
0
- 1
Vacuum Vessel
Av
S1
2*Ac
Electrode
H3
H1
H2
- 3
- 2
- 1
0
1
2
3
Normalized Distance (X Axis)

Fig.1 a

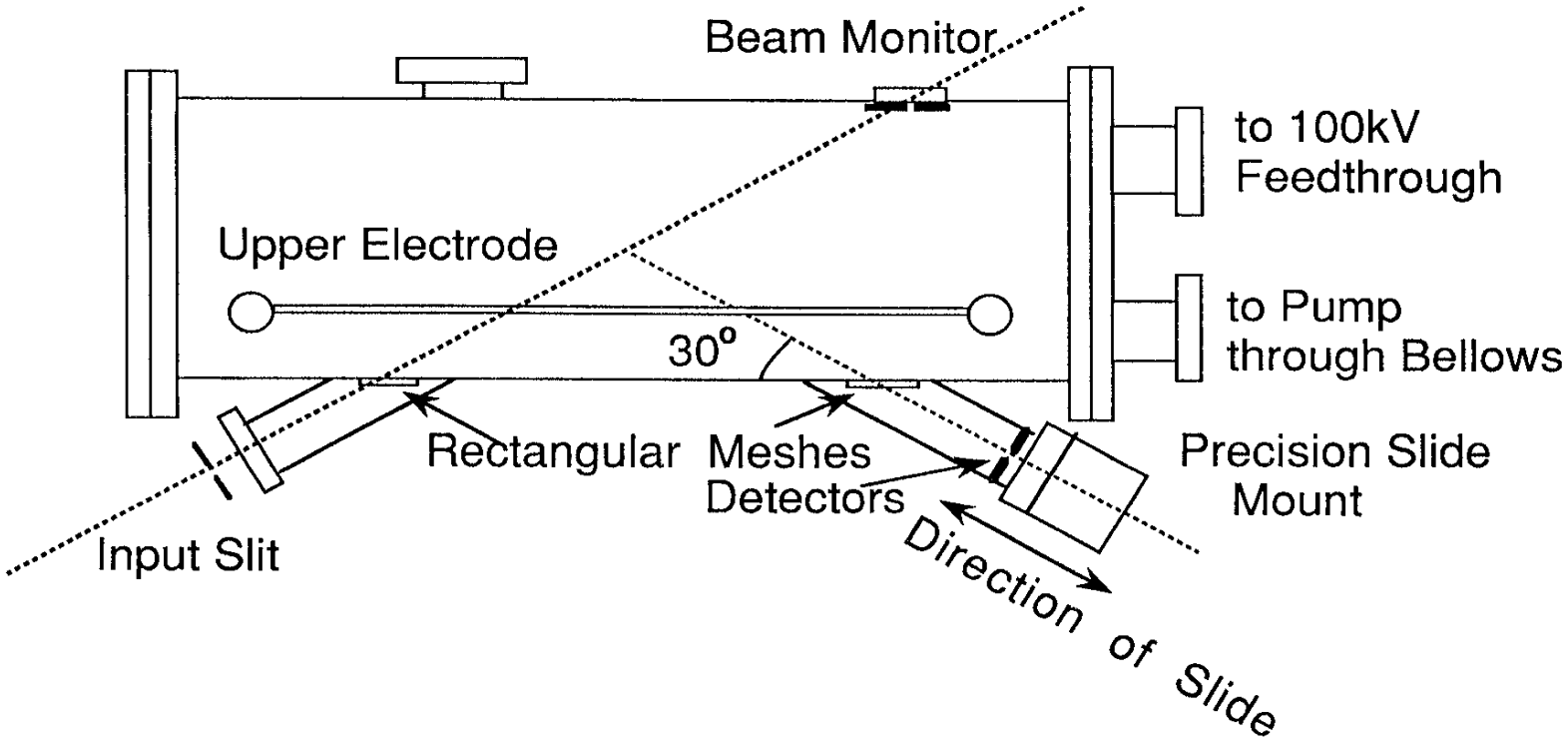
Beam Monitor
to 100kV
Feedthrough
Upper Electrode
to Pump
through Bellows
30°
Rectangular Meshes
Detectors
Precision Slide
Mount
Input Slit
Direction of Slide

Fig.1 b

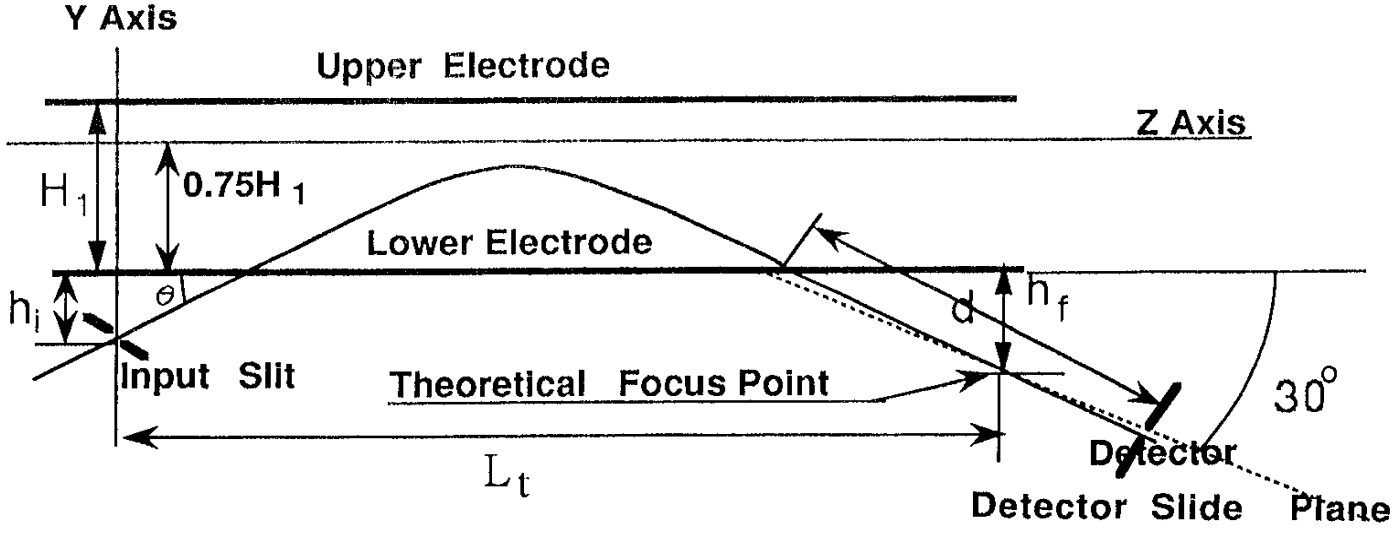
Y Axis
Upper Electrode
Z Axis
H 1
0.75H 1
Lower Electrode
h i
θ
d
h f
Input Slit
Theoretical Focus Point
30°
L t
Detector
Detector Slide
Plane

Fig.2

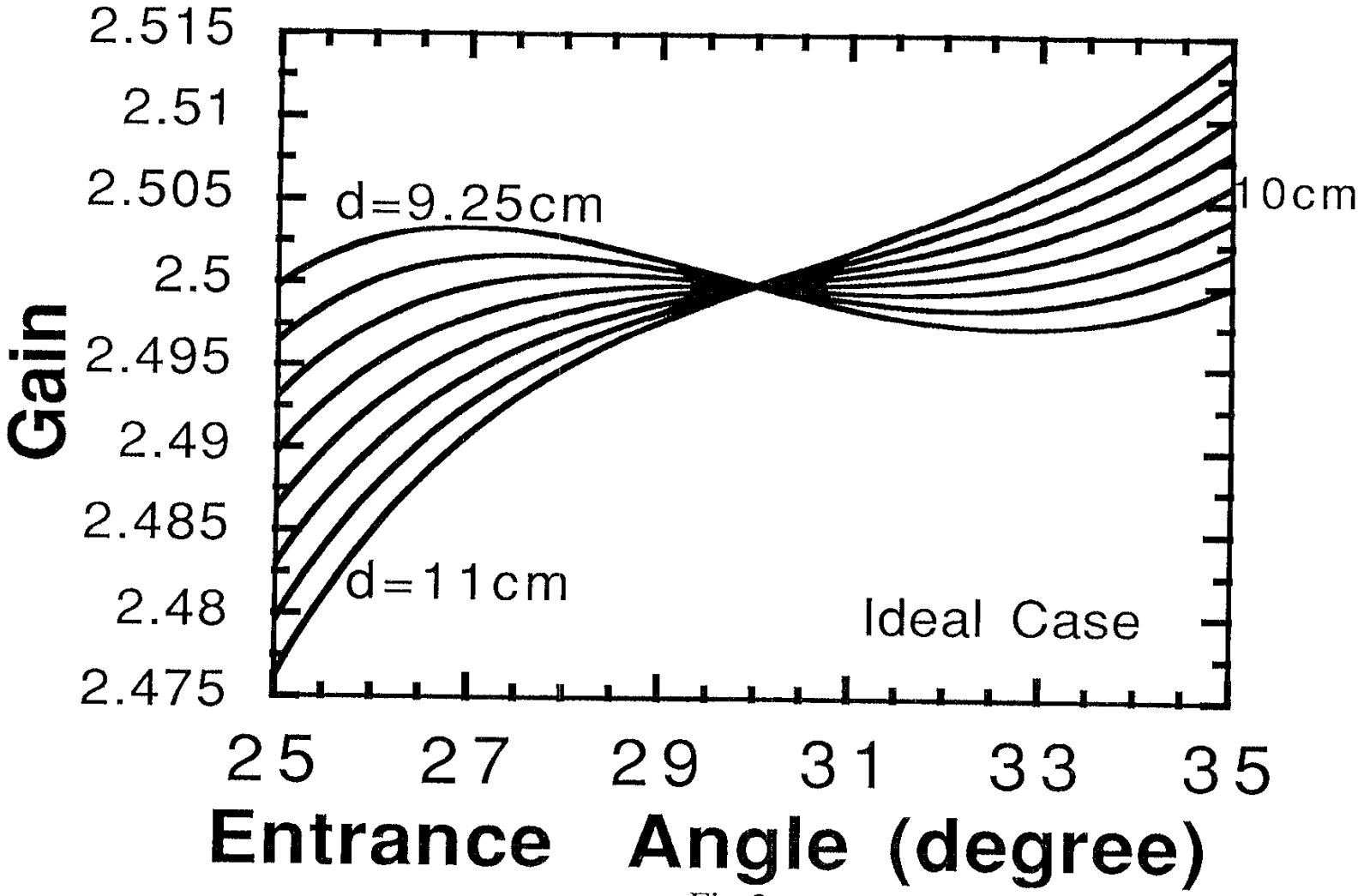
2.515
2.51
2.505
2.5
2.495
2.49
2.485
2.48
2.475
Gain
d=9.25cm
10cm
d=11cm
Ideal Case
25
27
29
31
33
35
Entrance Angle (degree)

Fig.3

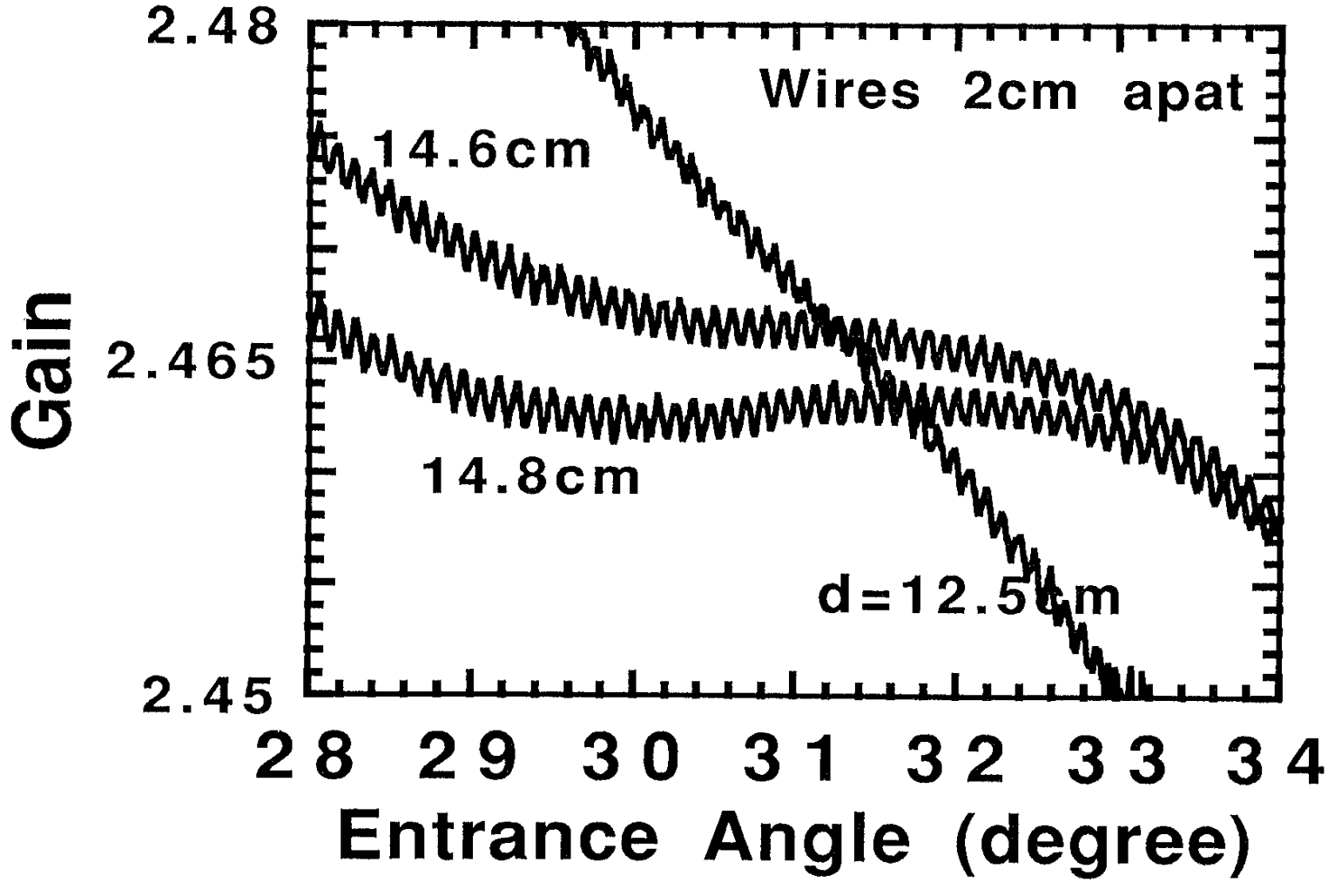
2.48
2.465
2.45
Gain
Wires 2cm apat
14.6cm
14.8cm
d=12.5cm
28 29 30 31 32 33 34
Entrance Angle (degree)

Fig.4

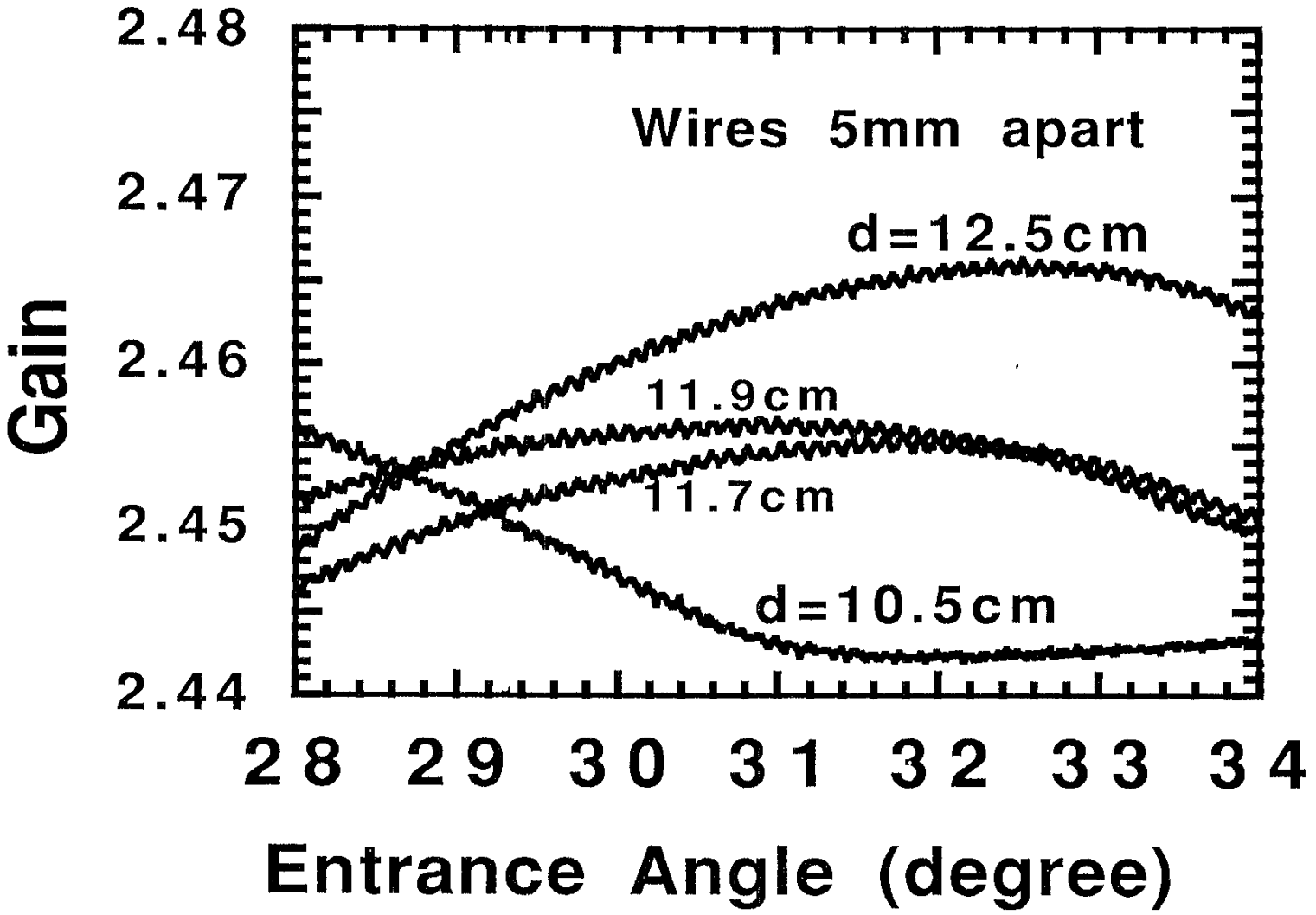
Wires 5mm apart
d=12.5cm
11.9cm
11.7cm
d=10.5cm
Gain
2.48
2.47
2.46
2.45
2.44
28 29 30 31 32 33 34
Entrance Angle (degree)

Fig.5

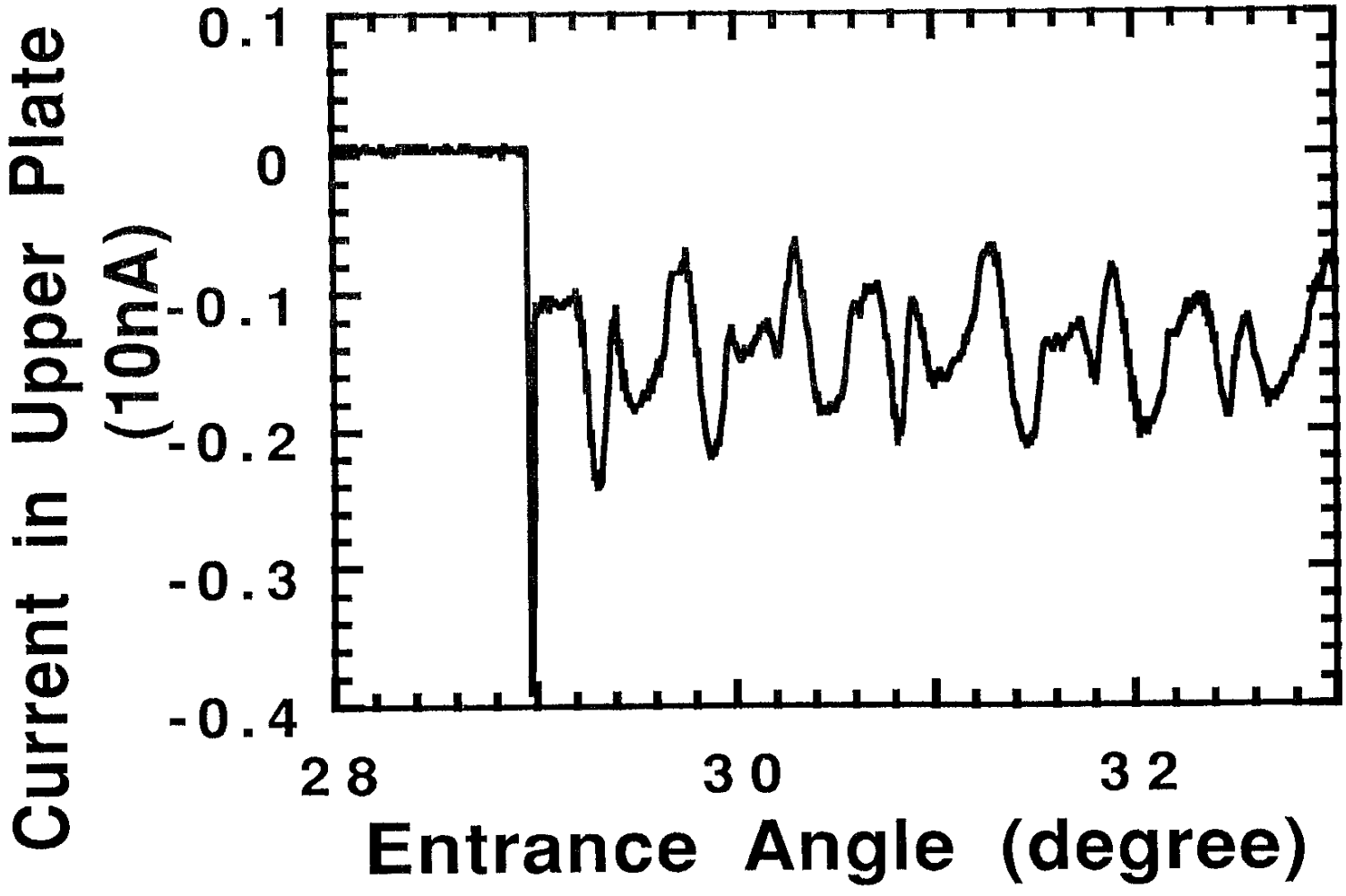
Current in Upper Plate (10nA)
0.1
0
-0.1
-0.2
-0.3
-0.4
28
30
32
Entrance Angle (degree)

Fig.6 (a)

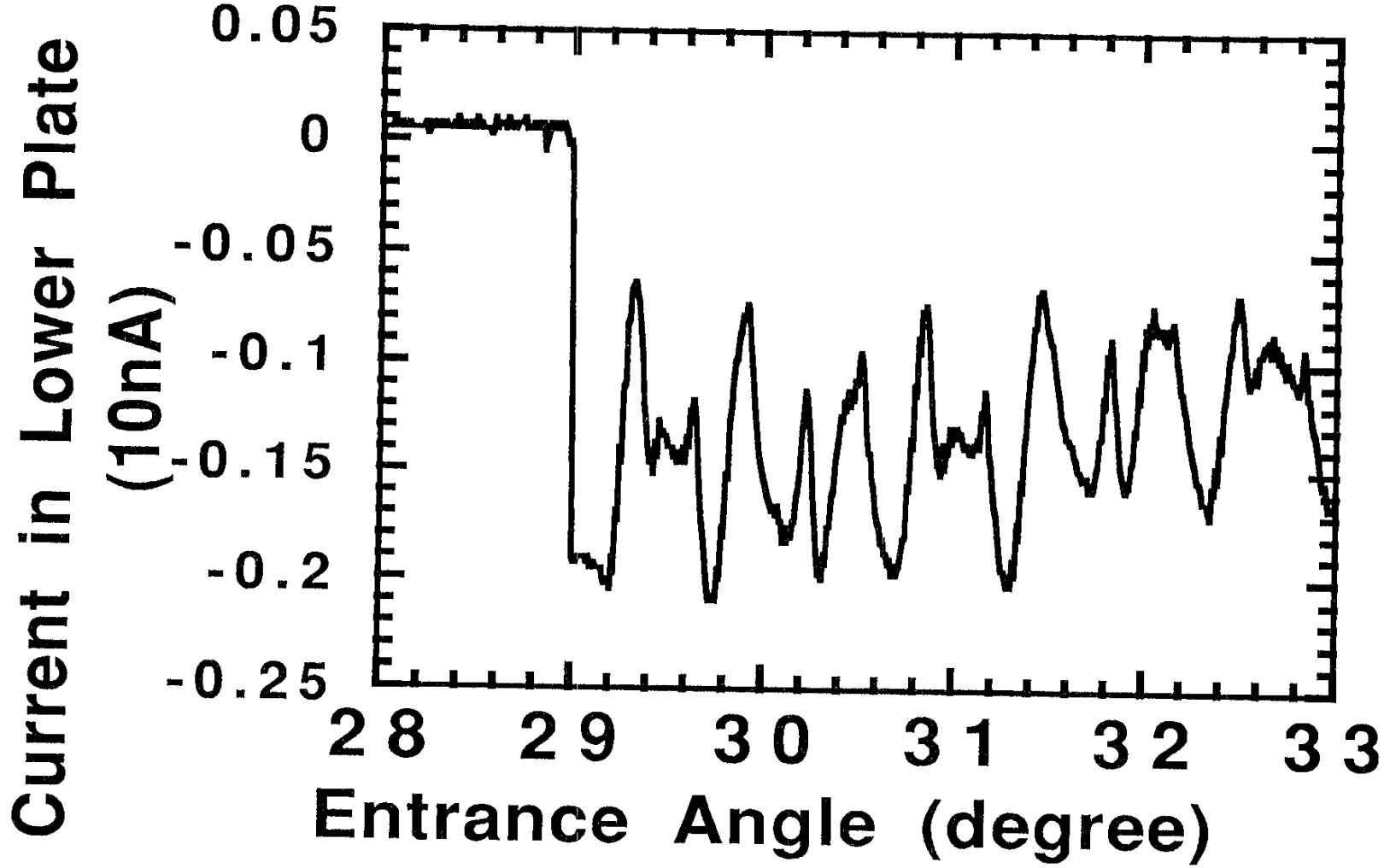
Current in Lower Plate
(10nA)
0.05
0
-0.05
-0.1
-0.15
-0.2
-0.25
28
29
30
31
32
33
Entrance Angle (degree)

Fig.6 (b)

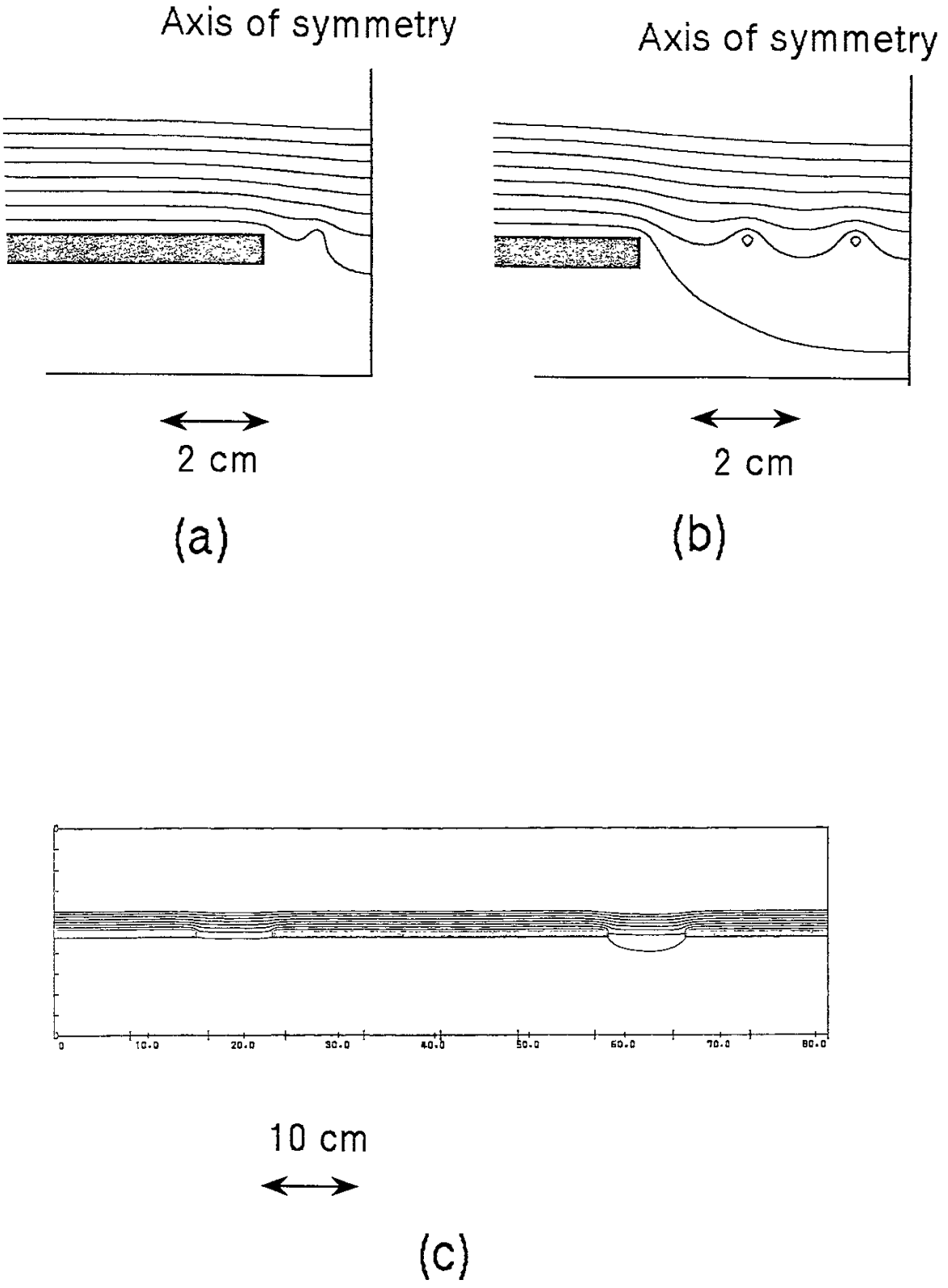
Axis of symmetry
Axis of symmetry
2 cm
2 cm
(a)
(b)
0
10.0
20.0
30.0
40.0
50.0
60.0
70.0
80.0
10 cm
(c)

Fig.7

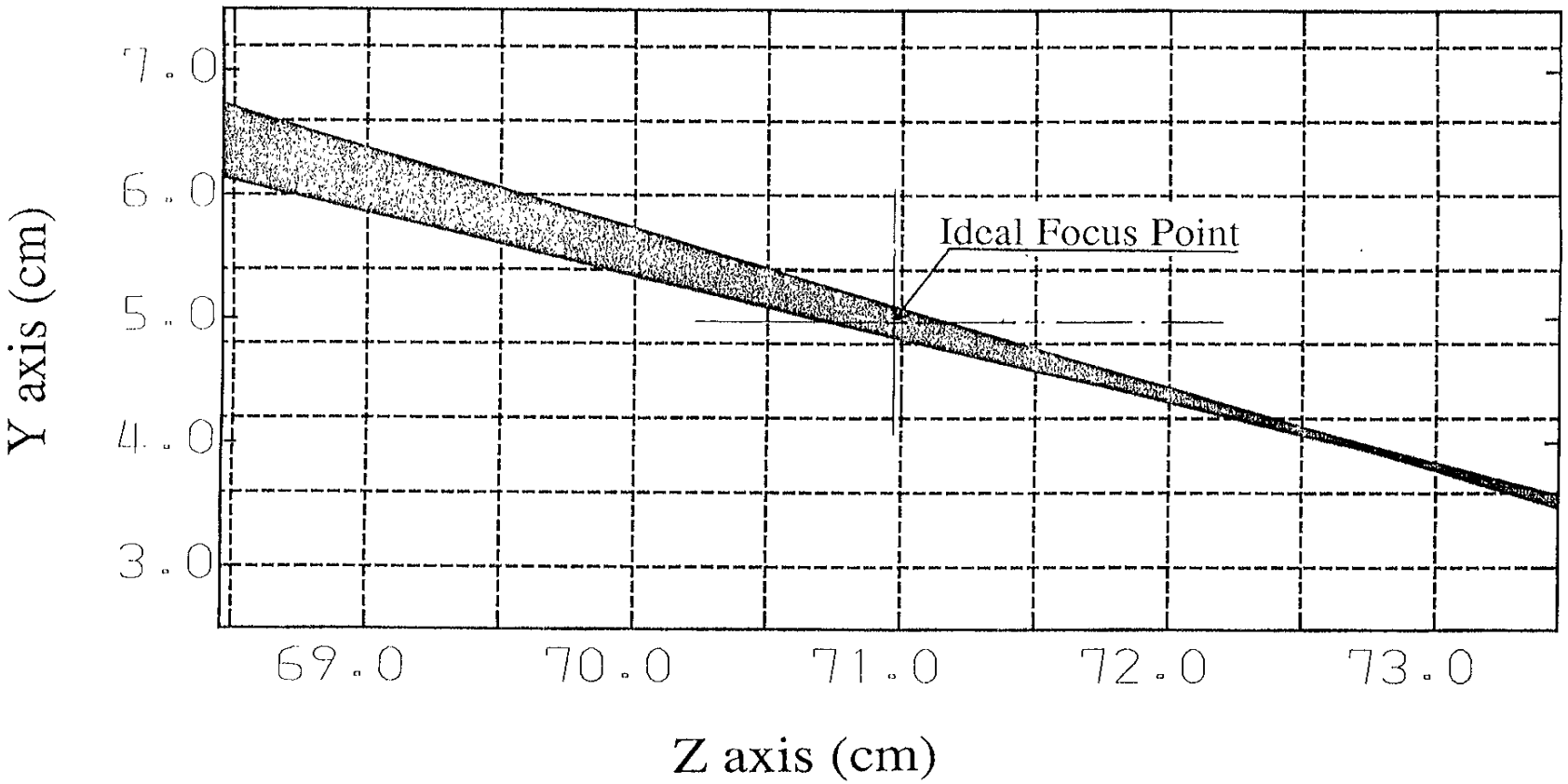
Y axis (cm)
7.0
6.0
5.0
4.0
3.0
Ideal Focus Point
69.0
70.0
71.0
72.0
73.0
Z axis (cm)

Fig.8

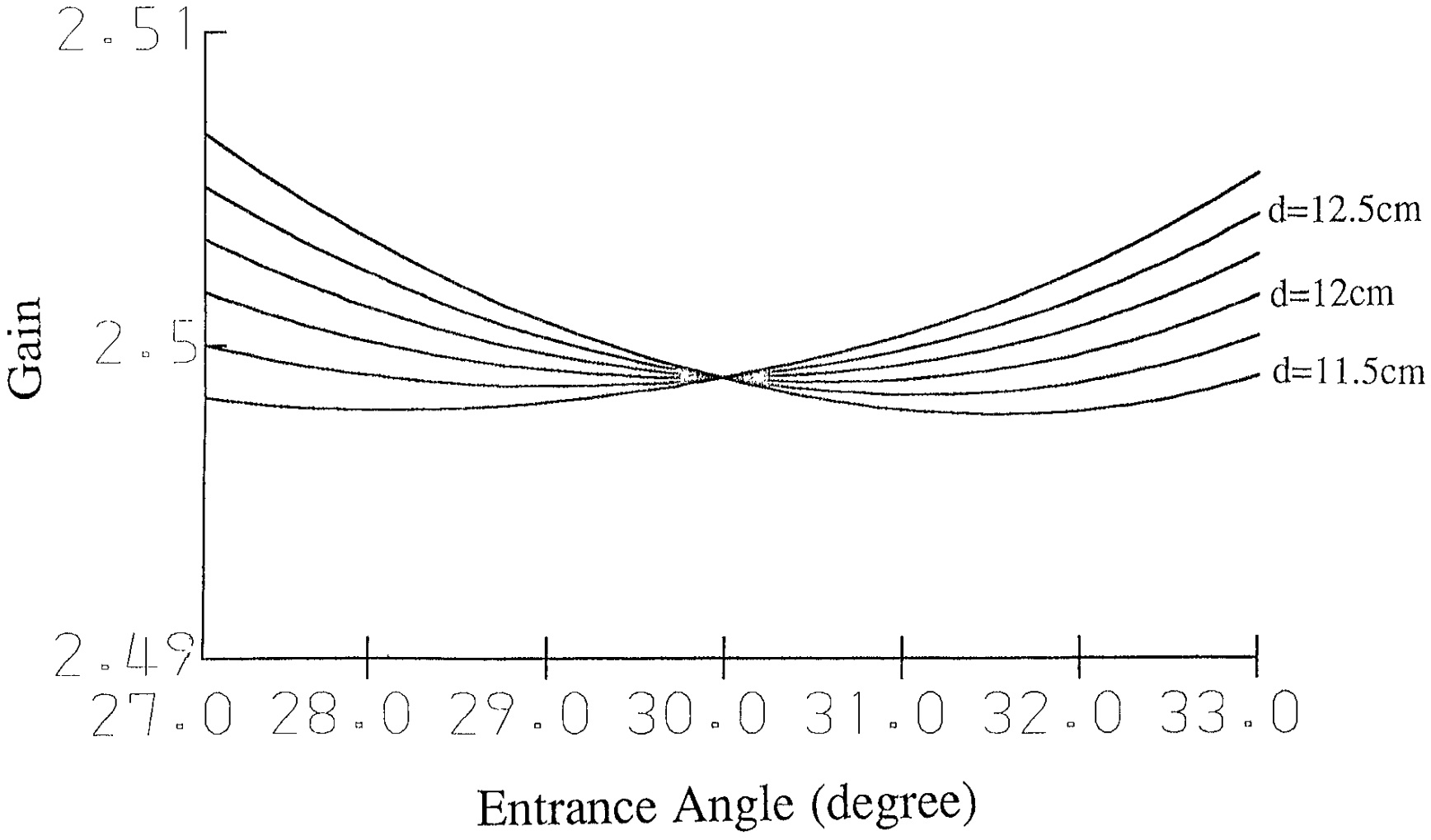
2.51
2.5
2.49
Gain
d=12.5cm
d=12cm
d=11.5cm
27.0 28.0 29.0 30.0 31.0 32.0 33.0
Entrance Angle (degree)

Fig.9 a

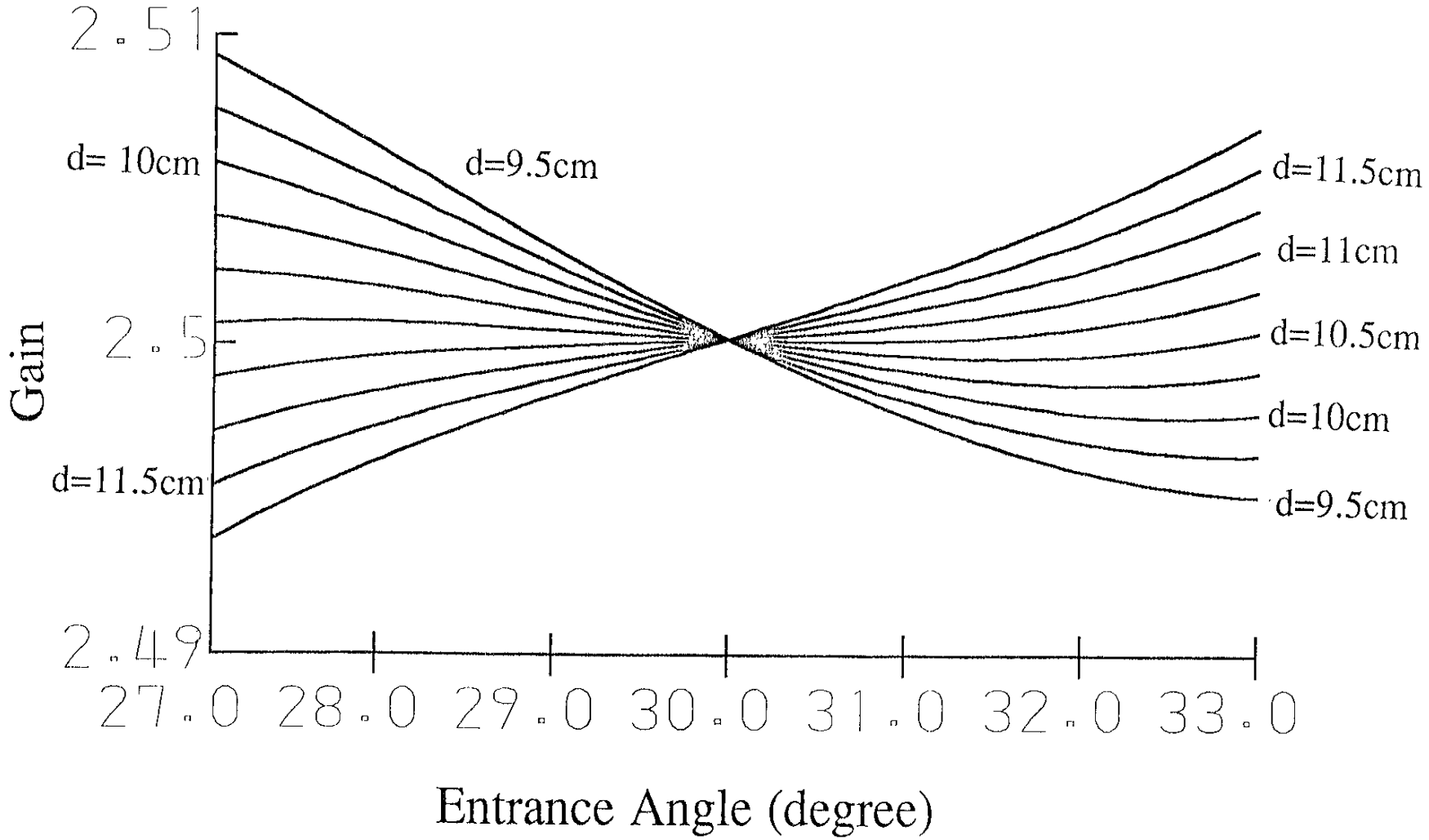
2.51
d= 10cm
d=9.5cm
d=11.5cm
d=11cm
d=10.5cm
d=10cm
d=9.5cm
Gain
2.5
d=11.5cm
2.49
27.0 28.0 29.0 30.0 31.0 32.0 33.0
Entrance Angle (degree)

Fig.9 b

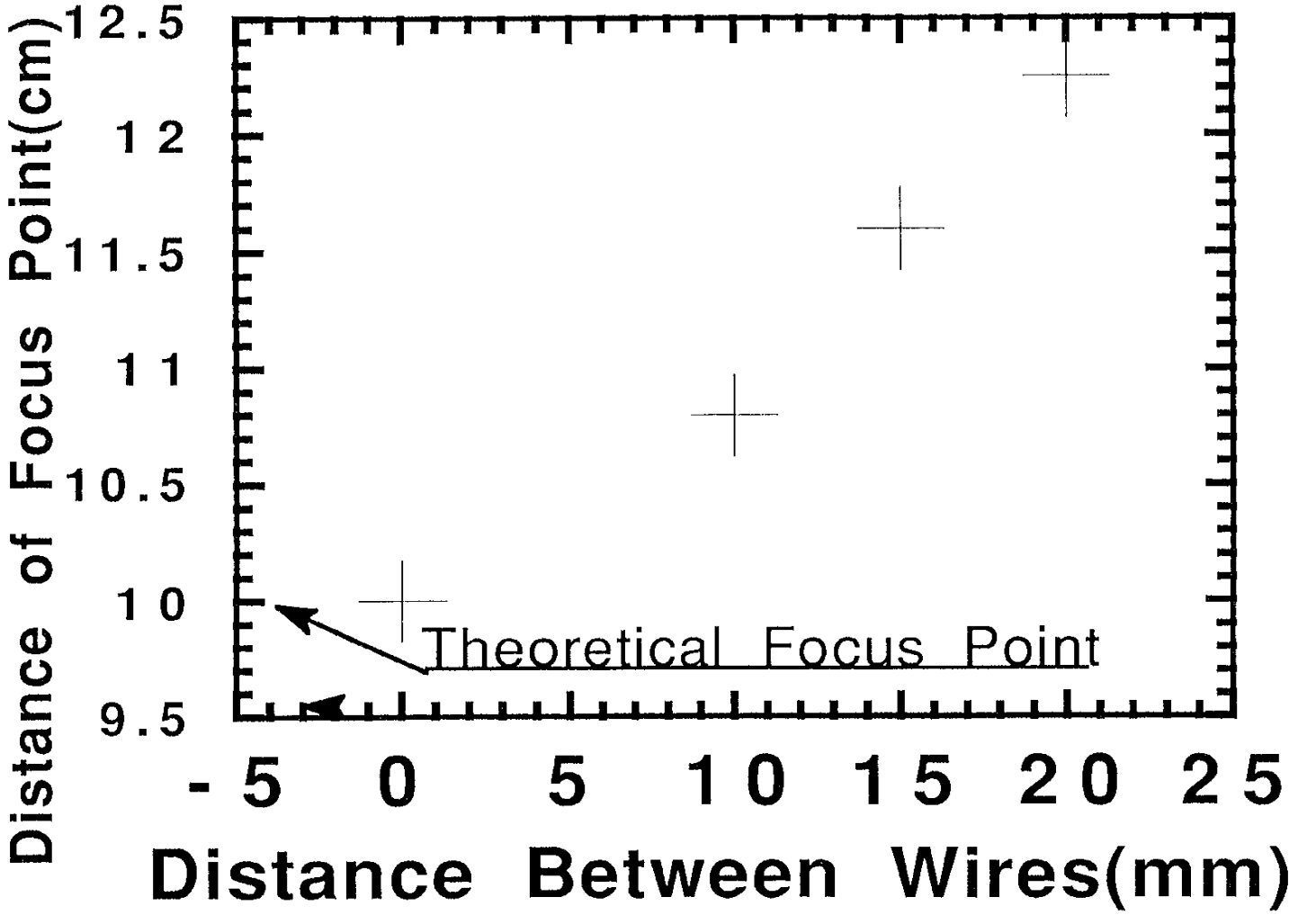
Distance of Focus Point(cm)
12.5
12
11.5
11
10.5
10
9.5
Theoretical Focus Point
-5 0 5 10 15 20 25
Distance Between Wires(mm)

Fig.10

Recent Issues of NIFS Series

NIFS-162 V. D. Pustovitov, *Refined Theory of Diamagnetic Effect in Stellarators;* Aug. 1992

NIFS-163 K. Itoh, *A Review on Application of MHD Theory to Plasma Boundary Problems in Tokamaks*; Aug. 1992

NIFS-164 Y.Kondoh and T.Sato, *Thought Analysis on Self-Organization Theories of MHD Plasma*; Aug. 1992

NIFS-165 T. Seki, R. Kumazawa, T. Watari, M. Ono, Y. Yasaka, F. Shimpo, A. Ando, O. Kaneko, Y. Oka, K. Adati, R. Akiyama, Y. Hamada, S. Hidekuma, S. Hirokura, K. Ida, A. Karita, K. Kawahata, Y. Kawasumi, Y. Kitoh, T. Kohmoto, M. Kojima, K. Masai, S. Morita, K. Narihara, Y. Ogawa, K. Ohkubo, S. Okajima, T. Ozaki, M. Sakamoto, M. Sasao, K. Sato, K. N. Sato, H. Takahashi, Y. Taniguchi, K. Toi and T. Tsuzuki, *High Frequency Ion Bernstein Wave Heating Experiment on JIPP T-IIU Tokamak*; Aug. 1992

NIFS-166 Vo Hong Anh and Nguyen Tien Dung, *A Synergetic Treatment of the Vortices Behaviour of a Plasma with Viscosity*; Sep. 1992

NIFS-167 K. Watanabe and T. Sato, *A Triggering Mechanism of Fast Crash in Sawtooth Oscillation*; Sep. 1992

NIFS-168 T. Hayashi, T. Sato, W. Lotz, P. Merkel, J. Nührenberg, U. Schwenn and E. Strumberger, *3D MHD Study of Helias and Heliotron;* Sep. 1992

NIFS-169 N. Nakajima, K. Ichiguchi, K. Watanabe, H. Sugama, M. Okamoto, M. Wakatani, Y. Nakamura and C. Z. Cheng, *Neoclassical Current and Related MHD Stability, Gap Modes, and Radial Electric Field Effects in Heliotron and Torsatron Plasmas;* Sep. 1992

NIFS-170 H. Sugama, M. Okamoto and M. Wakatani, *K- ε Model of Anomalous Transport in Resistive Interchange Turbulence* ; Sep, 1992

NIFS-171 H. Sugama, M. Okamoto and M. Wakatani, *Vlasov Equation in the Stochastic Magnetic Field* ; Sep. 1992

NIFS-172 N. Nakajima, M. Okamoto and M. Fujiwara, *Physical Mechanism of E_ψ-Driven Current in Asymmetric Toroidal Systems* ; Sep.1992

NIFS-173 N. Nakajima. J. Todoroki and M. Okamoto, *On Relation between Hamada and Boozer Magnetic Coordinate System* ; Sep. 1992

NIFS-174 K. Ichiguchi, N. Nakajima, M. Okamoto, Y. Nakamura and M. Wakatani, *Effects of Net Toroidal Current on Mercier Criterion in the Large Helical Device* ; Sep. 1992

NIFS-175 S. -I. Itoh, K. Itoh and A. Fukuyama, *Modelling of ELMs and Dynamic Responses of the H-Mode* ; Sep. 1992

NIFS-176 K. Itoh, S.-I. Itoh, A. Fukuyama, H. Sanuki, K. Ichiguchi and J. Todoroki, *Improved Models of β-Limit, Anomalous Transport and Radial Electric Field with Loss Cone Loss in Heliotron / Torsatron* ; Sep. 1992

NIFS-177 N. Ohyabu, K. Yamazaki, I. Katanuma, H. Ji, T. Watanabe, K. Watanabe, H. Akao, K. Akaishi, T. Ono, H. Kaneko, T. Kawamura, Y. Kubota, N. Noda, A. Sagara, O. Motojima, M. Fujiwara and A. Iiyoshi, *Design Study of LHD Helical Divertor and High Temperature Divertor Plasma Operation* ; Sep. 1992

NIFS-178 H. Sanuki, K. Itoh and S.-I. Itoh, *Selfconsistent Analysis of Radial Electric Field and Fast Ion Losses in CHS Torsatron / Heliotron* ; Sep. 1992

NIFS-179 K. Toi, S. Morita, K. Kawahata, K. Ida, T. Watari, R. Kumazawa, A. Ando, Y. Oka, K. Ohkubo, Y. Hamada, K. Adati, R. Akiyama, S. Hidekuma, S. Hirokura, O. Kaneko, T. Kawamoto, Y. Kawasumi, M. Kojima, T. Kuroda, K. Masai, K. Narihara, Y. Ogawa, S. Okajima, M. Sakamoto, M. Sasao, K. Sato, K. N. Sato, T. Seki, F. Shimpo, S. Tanahashi, Y. Taniguchi, T. Tsuzuki, *New Features of L-H Transition in Limiter H-Modes of JIPP T-IIU* ; Sep. 1992

NIFS-180 H. Momota, Y. Tomita, A. Ishida, Y. Kohzaki, M. Ohnishi, S. Ohi, Y. Nakao and M. Nishikawa, *D-^{3}He Fueled FRC Reactor "Artemis-L"* ; Sep. 1992

NIFS-181 T. Watari, R. Kumazawa, T. Seki, Y. Yasaka, A. Ando, Y. Oka, O. Kaneko, K. Adati, R. Akiyama, Y. Hamada, S. Hidekuma, S. Hirokura, K. Ida, K. Kawahata, T. Kawamoto, Y. Kawasumi, S. Kitagawa, M. Kojima, T. Kuroda, K. Masai, S. Morita, K. Narihara, Y. Ogawa, K. Ohkubo, S. Okajima, T. Ozaki, M. Sakamoto, M. Sasao, K. Sato, K. N. Sato, F. Shimpo, H. Takahashi, S. Tanahasi, Y. Taniguchi, K. Toi, T. Tsuzuki and M. Ono, *The New Features of Ion Bernstein Wave Heating in JIPP T-IIU Tokamak*; Sep, 1992

NIFS-182 K. Itoh, H. Sanuki and S.-I. Itoh, *Effect of Alpha Particles on Radial Electric Field Structure in Torsatron / Heliotron Reactor*; Sep. 1992

NIFS-183 S. Morimoto, M. Sato, H. Yamada, H. Ji, S. Okamura, S. Kubo,

O. Motojima, M. Murakami, T. C. Jernigan, T. S. Bigelow, A. C. England, R. S. Isler, J. F. Lyon, C. H. Ma, D. A. Rasmussen, C. R. Schaich, J. B. Wilgen and J. L. Yarber, *Long Pulse Discharges Sustained by Second Harmonic Electron Cyclotron Heating Using a $35GH_Z$ Gyrotron in the Advanced Toroidal Facility*; Sep. 1992

NIFS-184 S. Okamura, K. Hanatani, K. Nishimura, R. Akiyama, T. Amano, H. Arimoto, M. Fujiwara, M. Hosokawa, K. Ida, H. Idei, H. Iguchi, O. Kaneko, T. Kawamoto, S. Kubo, R. Kumazawa, K. Matsuoka, S. Morita, O. Motojima, T. Mutoh, N. Nakajima, N. Noda, M. Okamoto, T. Ozaki, A. Sagara, S. Sakakibara, H. Sanuki, T. Seki, T. Shoji, F. Shimbo, C. Takahashi, Y. Takeiri, Y. Takita, K. Toi, K. Tsumori, M. Ueda, T. Watari, H. Yamada and I. Yamada, *Heating Experiments Using Neutral Beams with Variable Injection Angle and ICRF Waves in CHS* ; Sep. 1992

NIFS-185 H. Yamada, S. Morita, K. Ida, S. Okamura, H. Iguchi, S. Sakakibara, K. Nishimura, R. Akiyama, H. Arimoto, M. Fujiwara, K. Hanatani, S. P. Hirshman, K. Ichiguchi, H. Idei, O. Kaneko, T. Kawamoto, S. Kubo, D. K. Lee, K. Matsuoka, O, Motojima, T. Ozaki, V. D. Pustovitov, A. Sagara, H. Sanuki, T. Shoji, C. Takahashi, Y. Takeiri, Y. Takita, S. Tanahashi, J. Todoroki, K. Toi, K. Tsumori, M. Ueda and I. Yamada, *MHD and Confinement Characteristics in the High-β Regime on the CHS Low-Aspect-Ratio Heliotron / Torsatron* ; Sep. 1992

NIFS-186 S. Morita, H. Yamada, H. Iguchi, K. Adati, R. Akiyama, H. Arimoto, M. Fujiwara, Y. Hamada, K. Ida, H. Idei, O. Kaneko, K. Kawahata, T. Kawamoto, S. Kubo, R. Kumazawa, K. Matsuoka, T. Morisaki, K. Nishimura, S. Okamura, T. Ozaki, T. Seki, M. Sakurai, S, Sakakibara, A. Sagara, C. Takahashi, Y. Takeiri, H. Takenaga, Y. Takita, K. Toi, K. Tsumori, K. Uchino, M. Ueda, T. Watari, I. Yamada, *A Role of Neutral Hydrogen in CHS Plasmas with Reheat and Collapse and Comparison with JIPP T-IIU Tokamak Plasmas* ; Sep. 1992

NIFS-187 K. Ioth, S.-I. Itoh, A. Fukuyama, M. Yagi and M. Azumi, *Model of the L-Mode Confinement in Tokamaks* ; Sep. 1992

NIFS-188 K. Itoh, A. Fukuyama and S.-I. Itoh, *Beta-Limiting Phenomena in High-Aspect-Ratio Toroidal Helical Plasmas*; Oct. 1992

NIFS-189 K. Itoh, S. -I. Itoh and A. Fukuyama, *Cross Field Ion Motion at Sawtooth Crash* ; Oct. 1992

NIFS-190 N. Noda, Y. Kubota, A. Sagara, N. Ohyabu, K. Akaishi, H. Ji, O. Motojima, M. Hashiba, I. Fujita, T. Hino, T. Yamashina, T. Matsuda, T. Sogabe, T. Matsumoto. K. Kuroda, S. Yamazaki, H. Ise, J. Adachi and T. Suzuki, *Design Study on Divertor Plates of Large Helical Device*

(LHD) ; Oct. 1992

NIFS-191 Y. Kondoh, Y. Hosaka and K. Ishii, *Kernel Optimum Nearly-Analytical Discretization (KOND) Algorithm Applied to Parabolic and Hyperbolic Equations* : Oct. 1992

NIFS-192 K. Itoh, M. Yagi, S.-I. Itoh, A. Fukuyama and M. Azumi, *L-Mode Confinement Model Based on Transport-MHD Theory in Tokamaks* ; Oct. 1992

NIFS-193 T. Watari, *Review of Japanese Results on Heating and Current Drive* ; Oct. 1992

NIFS-194 Y. Kondoh, *Eigenfunction for Dissipative Dynamics Operator and Attractor of Dissipative Structure* ; Oct. 1992

NIFS-195 T. Watanabe, H. Oya, K. Watanabe and T. Sato, *Comprehensive Simulation Study on Local and Global Development of Auroral Arcs and Field-Aligned Potentials* ; Oct. 1992

NIFS-196 T. Mori, K. Akaishi, Y. Kubota, O. Motojima, M. Mushiaki, Y. Funato and Y. Hanaoka, *Pumping Experiment of Water on B and LaB_6 Films with Electron Beam Evaporator* ; Oct., 1992

NIFS-197 T. Kato and K. Masai, *X-ray Spectra from Hinotori Satellite and Suprathermal Electrons* ; Oct. 1992

NIFS-198 K. Toi, S. Okamura, H. Iguchi, H. Yamada, S. Morita, S. Sakakibara, K. Ida, K. Nishimura, K. Matsuoka, R. Akiyama, H. Arimoto, M. Fujiwara, M. Hosokawa, H. Idei, O. Kaneko, S. Kubo, A. Sagara, C. Takahashi, Y. Takeiri, Y. Takita, K. Tsumori, I. Yamada and H. Zushi, *Formation of H-mode Like Transport Barrier in the CHS Heliotron / Torsatron* ; Oct. 1992

NIFS-199 M. Tanaka, *A Kinetic Simulation of Low-Frequency Electromagnetic Phenomena in Inhomogeneous Plasmas of Three-Dimensions* ; Nov. 1992

NIFS-200 K. Itoh, S.-I. Itoh, H. Sanuki and A. Fukuyama, *Roles of Electric Field on Toroidal Magnetic Confinement*, Nov. 1992

NIFS-201 G. Gnudi and T. Hatori, *Hamiltonian for the Toroidal Helical Magnetic Field Lines in the Vacuum*; Nov. 1992

NIFS-202 K. Itoh, S.-I. Itoh and A. Fukuyama, *Physics of Transport Phenomena in Magnetic Confinement Plasmas*; Dec. 1992